PHYSICAL REVIEW B **109**, 064104 (2024)

Temperature dependence of electric-field gradient in Zn and Cd: Replacing the $T^{3/2}$ law

H. Haas [*]
Department of Physics and CICECO, University of Aveiro, 3810-193 Aveiro, Portugal
and EP Division, CERN, 1211 Geneve-23, Switzerland

(Received 8 September 2022; revised 8 December 2023; accepted 12 December 2023; published 13 February 2024)

The existing experimental data for the temperature dependence of the nuclear quadrupole interaction in Zn and Cd have been accounted for by considering reanalyzed data for structure and vibrational amplitude as a function of temperature, in combination with density functional calculations of the electric-field gradient (EFG) variation due to the structure change. For Zn the complex EFG temperature effect, previously unexplained, can be fully reproduced, while for Cd it is shown that the apparent agreement with an earlier proposed universal temperature dependence as proportional to $T^{3/2}$ is due to a combination of structural and vibrational contributions. It is demonstrated that for Zn, in particular, the resulting EFG at 0 K, including the now directly calculated shift due to zero-point vibrations, and the subsequently obtained nuclear quadrupole moments, can be considerably different when taking the present revised analysis and all experimental data into account. As an additional example also one impurity system, ^{69}Ge in Zn, is tentatively analyzed in this context. The possible extension of the present approach to other noncubic s-p metals is envisioned.

DOI: 10.1103/PhysRevB.109.064104

I. INTRODUCTION

The study of the interaction of nuclear quadrupole moments (Q) with the surrounding charges can give detailed insight into the electronic distribution that creates bonding in solids. Following the discovery of nuclear quadrupole resonance (NQR) in the middle of the last century [1] and also the qualitative understanding of the temperature effects involved [2], a great number of experimental and theoretical studies of molecular and ionic solids have been performed. The electric-field gradients (EFGs) V_{zz}, the second derivative of the electric potential at the nuclear site, that determine the quadrupole interaction frequency $\nu_Q = eQV_{zz}/h$, have thus been interpreted quite early in a semiquantitative manner.

For metallic solids, on the other hand, the application of a radio-frequency technique like NQR is severely limited due to the rf skin effect and therefore only very few systems could be successfully investigated. With the introduction of perturbed angular correlation (PAC) [3] and perturbed angular distribution (PAD) [4] spectroscopy in the early 1970s these limitations have disappeared. In addition, such nuclear methods also allow the study of impurities even at extreme dilution. Thus, from about 50 years ago, an abundant amount of experimental information on the nuclear quadrupole interaction in metals has quickly been obtained [5]. It has become evident, however, that the electronic structure theory techniques available at the time were not appropriate for a reliable quantitative calculation of the EFG even in simple s-p metals. Thus, for interpreting the experimental results, also the EFG temperature dependence, recourse to semiquantitative approximations had to be accepted.

A large-scale systematic study of the EFG (here for simplicity called q as common in atomic physics) temperature dependence [6], however, had come up with a uniform description of a suggested "law" as $\Delta q(T)$ very closely proportional to $T^{3/2}$. This dependence apparently had so much appeal that it was later used in practically all cases, thus implying that lattice vibrations were the only effective sources. Other attempts to account for the EFG temperature dependence correctly tried to incorporate the structure and vibration changes [7–9] in their approach. These, however, could not reproduce the experimental data in detail, quantitative electronic structure calculations for the EFG not being possible at the time.

The situation changed dramatically with the availability of reliable density functional calculations also for metals [10,11]. Such techniques were actually used in two recent theoretical attempts in accounting for the EFG in Cd and Zn as a function of temperature [12,13]. Unfortunately, these treatments were concentrating on the effect of lattice vibrations only, apparently stimulated by the $T^{3/2}$ "law."

The present investigation was triggered by the observation that measurements of the EFG for Cd in Zn [14,15] using the excited $5/2^+$ state of ^{111}Cd at 245.4 keV with a half-life of 85.5 ns, had demonstrated a temperature dependence grossly different from the $T^{3/2}$ expectation. The purpose here is to include the changes of the EFG as a function of the well-known lattice parameters in the treatment by the now possible essentially quantitative calculations. This is then combined with an analysis of the experimental data available for the lattice vibration amplitudes as a function of temperature for

---

[*] heinz.haas@cern.ch

TABLE I. Parameters for the volume fit.

	V_{at} (0) (Å^3)	Θ_V (K)	$v_1 \times 10^2$	$v_2 \times 10^2$	$v_3 \times 10^2$
Zn	14.88154	314.5666	6.1550	–0.0303	0.7190
Cd	20.98244	185.7097	4.8874	0.7015	0.2598

Zn and Cd. A practically exact description of the existing experimental ν_Q frequency data in Zn and Cd hosts is arrived at by combining these two effects using one multiplicative fit parameter.

The thus developed quantitative approach to separate structural and motional contributions to the EFG temperature dependence, a property (at least in principle) exactly measurable with frequency accuracy, offers the possibility to get precise information on thermal vibration amplitudes in other noncubic metals, where such information is difficult to obtain with conventional methods.

II. STRUCTURAL INPUT DATA

The structural parameters for the hcp metals Zn and Cd, lattice volume (V), and ratio of the crystal axes length c to a (c/a), have in principle been available as a function of temperature for a long time. Though these are clearly the best-studied noncubic metals for these properties, there are still some uncertainties in the published literature. Since, in particular, the methods employed at low and high temperature were apparently never combined in a uniform way, a first reanalysis has been performed to obtain an internally consistent analytical description over the whole temperature range.

For lower temperatures, in particular, the thermal expansion data generally have a precision much superior to the measurements using x rays. They have, however, to be normalized to the "standard" lattice constants at ambient temperature. In addition, the well-known effect that, at temperatures in the region of melting, point defects thermally present in the crystal can change the lattice parameters [16] is very small and thus irrelevant for the present analysis.

The temperature-dependent atomic volumina, for these cases half the unit cell volumes, were described by functions of the type

$$V_{\mathrm{at}}(T) = V_{\mathrm{at}}(0)[1 + d_V(T)], \tag{1}$$

with

$$d_V(T) = \exp\left(-0.25\Theta_V/T\right)[v_1(T/T_{\mathrm{mp}}) + v_2(T/T_{\mathrm{mp}})^2 + v_3(T/T_{\mathrm{mp}})^3], \tag{2}$$

using the parameters presented in Table I. The volume expansion coefficients obtained in this way are practically identical over most of the temperature range to the ones calculated in [17] by using the conventional relation to heat capacity. They are, however, 3%–5% larger for temperatures around 50° below the melting point T_{mp}. Such discrepancies, presumably due to collective anharmonicity, are already known for other noncubic s-p metals (Be, Hg) [18,19]. Further careful analysis of all available information, compiled for the earlier work in [20], will be needed to confirm this observation. Initial results show that such effects only would alter the calculated EFG change due to the volume effect as used in this work by considerably less than 1%.

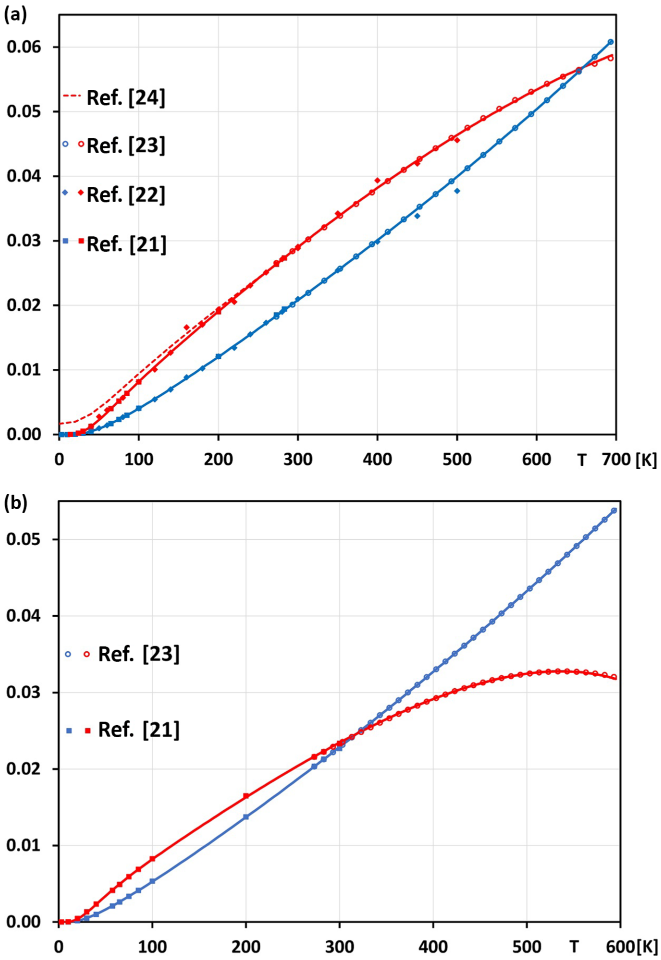

FIG. 1. (a) Change in c/a (absolute), in red, and volume (relative), in blue, for Zn. Reference numbers for the experimental data in square brackets (also in all further figures). The red dashed line shows the fit for c/a from Ref. [24]. (b) Change in c/a (absolute), in red, and volume (relative), in blue, for Cd.

For the variation of the c/a ratios a somewhat different functional form was found more appropriate as

$$c/a(T) = c/a(0) + d_{c/a}(T), \tag{3}$$

with

$$d_{c/a}(T) = c_1 d_V(T) + c_2 d_V(T)^2 + c_3\{1 - \exp[-d_V(T)d_3]\} + c_4 d_V(T)\exp[(T - T_{\mathrm{mp}})/\Theta_4]. \tag{4}$$

The last term was only necessary in the case of Cd to describe the extremely strong temperature dependence of c/a close to the melting point, but should undoubtedly also be there for Zn, albeit much smaller. Clearly other functional forms, perhaps physically better founded, would be conceivable to represent the experimentally measured c/a change. The present parametrization was only made to have a continuous numerical function closely representing the available experimental structure data.

In Figs. 1(a) and 1(b) the input data from early lattice expansion measurements below room temperature [21] and

TABLE II. Parameters for the c/a fit.

	$c/a(0)$	c_1	c_2	$c_3\times10^3$	d_3	$c_4\times10^3$	Θ_4 (K)
Zn	1.827683	1.3931	−7.98694	3.4992	365.0	0	
Cd	1.862580	1.1122	−8.43569	2.7491	535.9	−1.49	140

recent x-ray experiments for Zn [22], as well as a previous analysis for the high-temperature x-ray data [23], are combined to obtain the fit function parameters summarized in Table II. For Zn it should be noticed that another analysis of the c/a change in the low-temperature region exists [24], shown as a dashed line in Fig. 1(a), that extrapolates to a slightly different value at $T = 0$ from the one obtained here. Using this value, inconsistent with the x-ray data, would not change the analysis arrived at in the present work in any significant way, however.

III. DENSITY FUNCTIONAL CALCULATIONS FOR Cd AND Zn METAL

All solid-state calculations were performed with the full-potential linearized augmented plane waves code WIEN2K [25]. This program package has been known to yield accurate results for band structure and various properties for numerous solids, the precision mainly limited by the density functional (DF) used. It allows, in particular, for calculation of hyperfine interaction parameters at the nucleus, here EFG values, and the contributions of different orbitals. Standard technical parameters ($R_{\mathrm{MT}} = 2.3/2.7\, a_o$ (Zn/Cd); $l_{\max} = 10$; $k_{\max} = 9/R_{\mathrm{MT}}$; $G_{\max} = 12a_o^{-1}$; 455 k points in the reduced Brillouin zone) were used. The calculations were made in the scalar relativistic approximation, with an additional local d orbital to increase basis set flexibility and included the semicore p states for zinc and cadmium. Calculations for Cd included spin-orbit interaction to account for this (very small) contribution to the EFG. In the case of the hcp metals Cd and Zn a complication arises due to their complex band structure. This requires in principle a very dense mesh of k points, now possible in practical calculations with today's increased computing power. For the present DF calculations to determine the effect of changed volume and c/a ratio for Zn and Cd the generalized gradient approximation (PBE) [26] was employed. Calculations for the relative change of the EFG,

$$\delta(q/q_0) = [q(T) - -q(0)]/q(0), \tag{5}$$

(here using q for shortness) by varying the volume V with constant c/a gave

for Zn: $\delta(q/q_0)_{\mathrm{vol}} = -1.55(\Delta V/V_0)$;
for Cd: $\delta(q/q_0)_{\mathrm{vol}} = -1.61(\Delta V/V_0)$.

This implies a proportionality of the EFG to the volume with a Grüneisen-type exponent of about −1.6 for both metals.

Similarly, by varying c/a with constant volume the results are

for Zn: $\delta(q/q_0)_{c/a} = \Delta(c/a)/[c/a(0)–1.6172]$;
for Cd: $\delta(q/q_0)_{c/a} = \Delta(c/a)/[c/a(0)–1.5983]$.

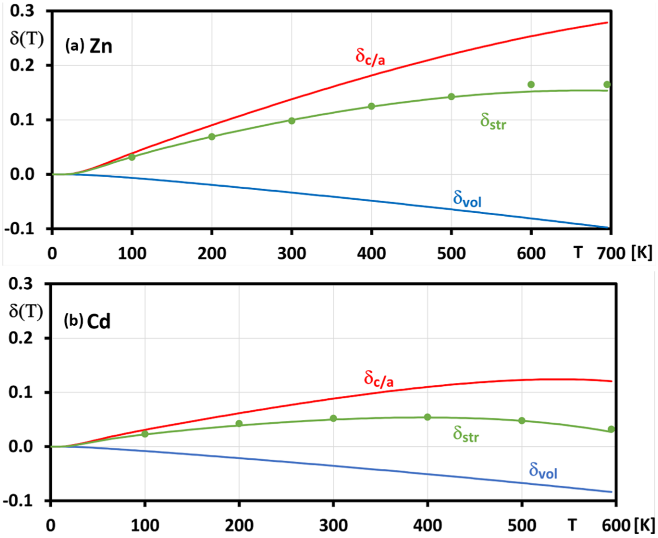

FIG. 2. Structural EFG changes as a function of temperature from DF calculations for (a) Zn and (b) Cd. The (green) points show the results of the direct calculations for the corresponding geometry.

This implies that for both metals the EFG does not extrapolate to zero at the ideal packing ratio for touching spheres of 1.633, but a somewhat smaller value.

Calculations with other standard functionals have shown that the results for the relative changes of the EFG, of primary concern in the present work, only change to a negligible extent. This must be compared to the fact that for the metals discussed here the absolute values calculated in this manner are typically 10%–15% smaller than the now available rather precise experimental values obtained with the corresponding, recently corrected, nuclear quadrupole moments [27–29]. In principle density functional calculations with the now available hybrid inclusion of Hartree-Fock exchange [30] have been shown to correct this deficiency [31], though with the effect of increasing the necessary computer resources by at least two orders of magnitude.

In Figs. 2(a) and 2(b) the calculated contributions to the EFG of the volume and c/a change, δ_{vol} and $\delta_{c/a}$, as a function of temperature obtained are shown, together with the combined structural effect δ_{str} leading to the structural relative EFG change as a function of temperature:

$$R_{\mathrm{str}}(T) = (1 + \delta_{\mathrm{str}}) = (1 + \delta_{\mathrm{vol}})(1 + \delta_{c/a}). \tag{6}$$

In addition, for the structure at several representative temperatures, calculations of the same type were performed. The obtained EFG changes, green dots in Figs. 2(a) and 2(b), are practically identical with those obtained by combining the two separately computed contributions.

It should be pointed out that the present calculations were only performed for the experimental structures of the bulk materials. Application of the results to an impurity system as the later treated case of Cd in Zn could introduce an additional uncertainty that would have been avoidable by supercell calculations including local lattice relaxation as, for example, performed in early *ab initio* calculations of the EFG for such cases [32]. Experimental studies of the EFG temperature effect had shown evidence, however, that for isovalent systems, like Cd in Zn, the observed dependence is very similar to the pure matrix one [6,33]. The simpler calculations, by orders of magnitude, performed here were thus considered a good approximation for the structural effect. The precision of this approach is demonstrated by the agreement also to the data for pure Zn discovered later as discussed below.

IV. VIBRATIONAL INPUT DATA

For the amplitudes of the thermal motion in the solid the experimentally significant numbers are the mean vibrational amplitudes $\langle x^2\rangle$ along a and $\langle z^2\rangle$ along c as a function of temperature. To obtain this information, in principle, accurate lattice diffraction experiments would be necessary. Due to the limited precision of the existing x-ray data (for Zn) and the nonavailability of accurate measurements over a large temperature range (for Cd) a somewhat different procedure was adopted here. For the present empirical analysis the use of the averaged vibrational amplitude Debye-Waller factor (DWF, here called B_{av} as common in x-ray work) was found sufficient: $B_{\text{av}} = (2B_x + B_z)/3$ with $B_x = 8\pi^2\langle x^2\rangle$ and $B_z = 8\pi^2\langle z^2\rangle$.

For Zn the very fortunate situation exists that experimental and theoretical data for the vibrational amplitudes are available from quite different approaches [34–36]. From there it is obvious that the most recent experimental data of [22] considerably overestimate the expected values in the low-temperature region. Various other theoretical calculations [37] lead to the same conclusion. On the other hand, the generally recommended vibrational amplitudes at room temperature for Zn [38], taken from [39], very slightly undershoot the function obtained below.

For Zn a fit function for the B factors [40] has recently been proposed as obtained by using only data from older x-ray experiments, combined with thermodynamic results. By adding a small term linear in T, typical for quasiharmonic contributions (though with an unphysical negative sign), and a fairly large T^3 term, accounting for nonharmonic contributions, this fit obtains close agreement with all now existing data as demonstrated in Fig. 3(a).

In the present work another approach is adopted that uses a physically more reasonable procedure and less adjustable parameters. In the classical investigations of the vibrational amplitudes as a function of temperature an analysis in terms of a temperature-dependent Debye temperature Θ was generally used [41]. At this time, however, only rough estimation of the temperature dependence of Θ was possible, the implicit assumption being that the effect of lattice expansion was reducing the vibrational frequencies governing Θ. With the present possibility of theoretical calculation of the lattice vibration frequencies [40] this approach could in principle be put on a quantitative basis, however. Unfortunately, no theoretical investigation of the volume dependence of the lattice frequencies for the hcp metals is available yet, but for fcc metals various such calculations exist. Results for Al [42], Cu [43], Ag [44], and others show that the frequency-volume dependence is close to the form $\omega/\omega_0 = (1+\delta_V)^{-\gamma}$, with the mode Grüneisen parameters γ in the region of 2–2.5. Taking such a dependence for Θ and a mode Grüneisen parameter of $\gamma_\Theta = 2.5$, the experimental excess of the vibrational amplitudes over the ones calculated using the low-temperature value of Θ, the dashed curve in Fig. 3(a), for Zn is virtually quantitatively accounted for. The data would only permit a quite small additional T^3 component characteristic for a pure nonharmonic contribution. The calculated trend of B_{av} obtained for a temperature-independent Θ without the thermal corrections is in complete agreement with the results of [45], obtained by using the data for the low-temperature vibration spectrum [46].

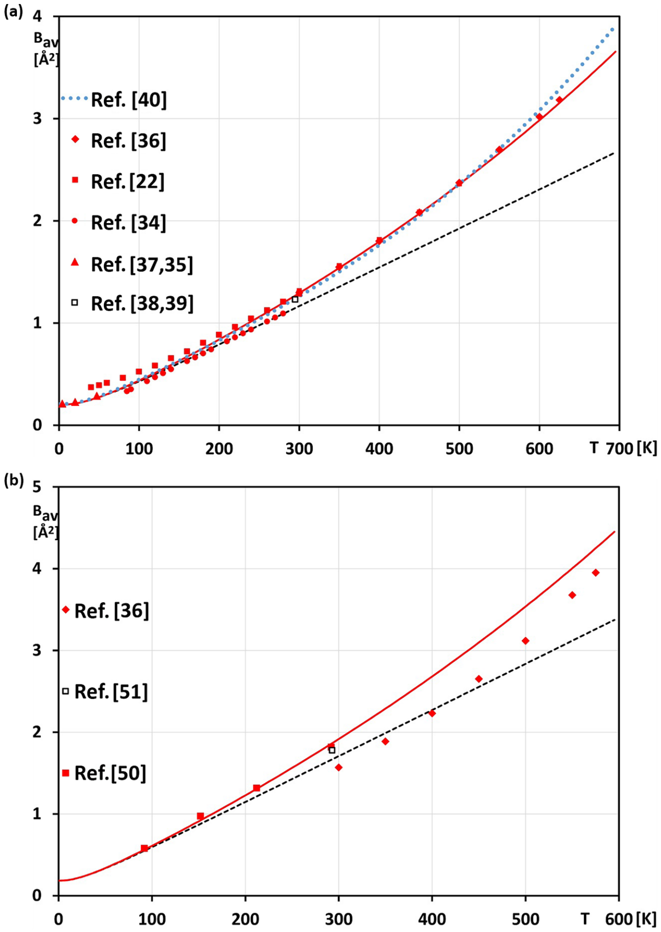

FIG. 3. (a) Average B factor for Zn. The strong red line shows the present fit, the dashed black line only the harmonic component. The dotted blue line is from the analysis of Ref. [40]. (b) Average B factor for Cd. The strong red line shows the present fit, the dashed black line only the harmonic component.

For Cd, as demonstrated in Fig. 3(b), the experimental situation would not warrant a fitted temperature dependence of B_{av}. Thus a completely theoretical approach has been taken by scaling the Debye temperatures to the ones for Zn simply via the experimentally known ratio of the lattice frequencies taken from phonon dispersion measurements using neutrons [47] for Zn and x rays [48] for Cd. The thus obtained ratio of $\Theta(\text{Zn})/\Theta(\text{Cd})$ of 1.58 is very close to the one generally used [49]. This approach, also assuming as the only thermal effect the Θ change due to the volume increase, brings B_{av} into full agreement with the limited experimental results of [50]. Again, the recommended vibrational amplitudes at room

TABLE III. Debye temperatures used to calculate the temperature-dependent B_{av}.

	Θ_a (K)	Θ_c (K)	γ_Θ
Zn	260.0	165.7	2.5
Cd	174.2	103.1	2.5

temperature [38], taken from [51], are very slightly lower than the ones obtained here. The dashed curve in Fig. 3(b), representing B_{av} without the thermal corrections, shows the same relation to the full results as for Zn, in complete disagreement with the here obviously wrong data of [36], obtained from measurements of only one x-ray reflex. It does, however, come very close to the theoretical results [52] obtained with the local density functional (LDA) that best reproduces the measured lattice frequencies [53].

It should be pointed out that the actual calculations for the contributions $\langle x^2\rangle$ and $\langle z^2\rangle$ were using quite different Debye temperatures Θ_a and Θ_c, given in Table III, as required for the highly anisotropic solids. For B_{av}, however, one would for the higher-temperature region obtain virtually identical results by using an averaged $\Theta_{\mathrm{av}} = 3^{1/2}(\Theta_c^{-2} + 2\Theta_a^{-2})^{-1/2}$.

V. CALCULATION PROCEDURE

Having the structural EFG change and B_{av} as a function of temperature, accepting the general assumption

$$q(\mathrm{T}) = q(0, \mathrm{st})\mathrm{R}_{\mathrm{tot}}(\mathrm{T}), \tag{7}$$

with $q(0, \mathrm{st})$ the EFG of the static nonvibrating system, the calculation procedure adopted is the following:

The structural and vibrational effects are taken as uncoupled,

$$R_{\mathrm{tot}}(T) = R_{\mathrm{str}}(T)R_{\mathrm{vib}}(T), \tag{8}$$

where $R_{\mathrm{str}}(T)$ is obtained from the DF calculations. For $R_{\mathrm{vib}}(T)$ a dependence on the average vibrational amplitude $B_{\mathrm{av}} = 8\pi^2(2\langle x^2\rangle + \langle z^2\rangle)/3$ is taken as

$$R_{\mathrm{vib}}(T) = \exp\left[-\beta_{\mathrm{av}}B_{\mathrm{av}}(T)/2\right], \tag{9}$$

in analogy to the usual Debye-Waller factor. This approximation follows [7] in ignoring an effect of the vibrational amplitude anisotropy. The proportionality factor β_{av} describing the EFG dependence on the average atomic displacements is in the present empirical treatment to be obtained from the experimental data for $q(T)$. The procedure could evidently be extended to be more general by including an anisotropic component,

$$B_{\mathrm{an}} = 8\pi^2(\langle z^2\rangle - \langle x^2\rangle), \tag{10}$$

with the obvious introduction of an additional parameter β_{an} (to be discussed below).

To account for the small effect of volume change with temperature and to be able to compare the different materials a renormalization of the vibrational amplitude was actually applied in the calculations as

$$B'_{\mathrm{av}}(T) = B_{\mathrm{av}}(T)/r_{\mathrm{nn}}(T)^2, \tag{11}$$

where the (effective) nearest neighbor distance r_{nn} is the calculated radius,

$$r_{\mathrm{nn}}^3 = (3/4\pi)\mathrm{V}_{\mathrm{at}}, \tag{12}$$

of a sphere with the (slightly temperature-dependent) volume per atom $V_{\mathrm{at}}(T)$ of the system. This results in a normalized dimensionless parameter $\beta\prime$ that should better reflect the effect of thermal motion and in addition also allow a rough comparison of materials.

Thus Eq. (9) in the final analysis of the experimental data is actually replaced by

$$R_{\mathrm{vib}}(T) = \exp[-\beta' B'_{\mathrm{av}}(T)/2]. \tag{13}$$

The corresponding proportionality parameter $\beta\prime$ is then simply determined by fitting the experimental data for $\nu_Q(T)/\nu_Q(0)$ to the calculated $R(T)/R(0)$, in practice generally taking $\nu_Q(0)$ equal to $\nu_Q(4\ \mathrm{K})$. Since $R(0)$ is always somewhat smaller than 1, this procedure then automatically also results in the zero-point vibration shift of ν_Q.

VI. ANALYSIS FOR ^{111}Cd PROBE IN Zn AND Cd DATA

The data for the relative temperature dependence $\nu_Q(T)/\nu_Q(4\,\mathrm{K})$ for ^{111}Cd in Zn are then only dependent on one parameter, $\beta\prime$. Using $\beta\prime = 0.47$ one obtains a virtually perfect fit to the available experimental measurements, as demonstrated in Fig. 4(a). The different contributions of the lattice structure and thermal motion effect that contribute to the final EFG are shown in Fig. 5(a). The “unusual” phenomenon of an EFG rising with temperature thus finds its totally natural explanation.

There is even another unexpected observation in the calculated EFG temperature dependence, the very slight initial dip in the data predicted around 25 K, shown as an inset on an enlarged scale in Fig. 5(a). This effect is apparently also visible in the experimental data of Fig. 4(a), though at the limit of statistical accuracy. There is also a hint of it in the Mössbauer measurements [35] for ^{57}Zn in Zn shown in Fig. 6, to be discussed below. It is the result of an interplay of the functional dependence of the structural and thermic contributions, originating from the fact that the vibrational amplitudes along a and c are changing differently at low temperatures.

On the contrary, the conspicuous drop of the experimental EFG below 10 K seen in Fig. 4(a) cannot be accounted for. There is in fact a well-known change of the experimental c/a ratio for Zn metal in this region [21]. Its measured amplitude, however, is much too small to account for the experimental dip within a simple structural explanation. Assuming that this other “unusual” phenomenon persists in a remeasurement, one would have to look for an electronic explanation, possibly originating as an “aftereffect” of the preceding nuclear decay.

The originally unexpected increase of ν_Q in the temperature region 50–200 K, well documented in the measurements of [14], may actually also be seen in the earlier PAC data of [54], but this work was never discussed in the present context.

In a similar way Fig. 4(b) shows the results for ^{111}Cd in Cd. Leaving out the obviously wrong temperatures taken for the initial PAC measurement [55] at higher T, in contradiction with all later work, and the well-documented discrepancy due to implantation damage in the PAD data [4] at low T, one can

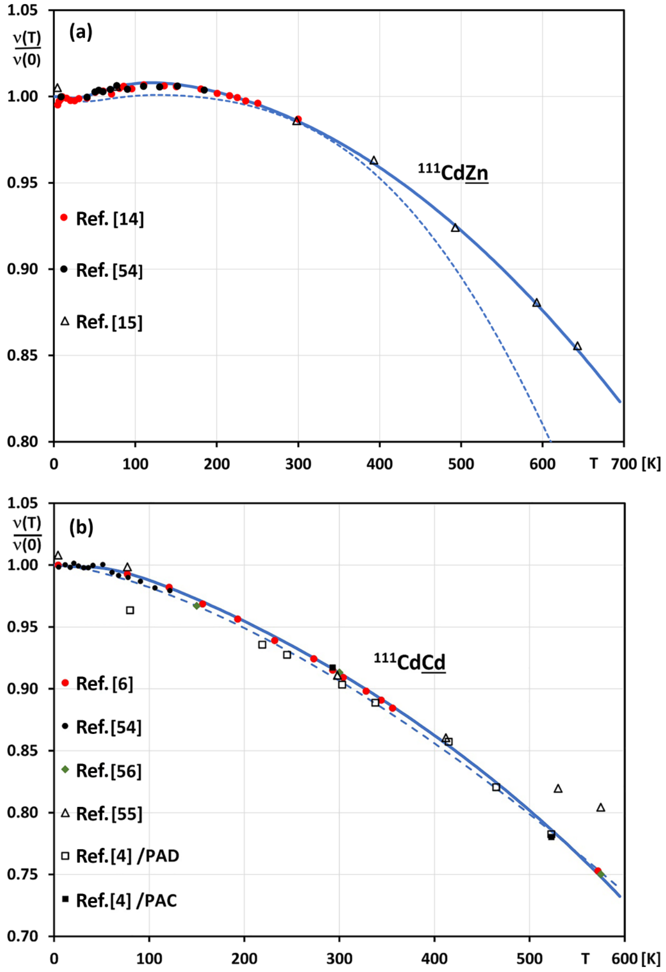

FIG. 4. (a) Experimental data for ^{111}Cd in Zn. The strong blue line shows the present fit, the dashed blue line a fit assuming proportionality to only the anisotropic B, using data from Ref. [40]. (b) Experimental data for ^{111}Cd in Cd. The strong blue line shows the present fit, the dashed blue line a fit proportional to $T^{3/2}$. The two high-temperature points from Ref. [55] and the PAD data below 300 K from Ref. [4] can safely be ignored.

see that the present approach does represent the data, including those from a pressure dependence study [56], extremely well, using $\beta' = 0.5$. Inspection of the different contributions in Fig. 5(b) makes it clear that the major effect of the observed curvature comes from the lattice change and not directly from the vibrational motion. The previously observed closeness of the data to a $T^{3/2}$ dependence, shown for comparison also in Fig. 4(b) as a dashed line, is thus merely an accident of nature.

VII. DISCUSSION

The here achieved essentially quantitative description of the EFG temperature dependence for Cd in Zn and Cd with the use of one parameter β' raises several questions:

(a) Is the separation of thermal and structural contribution justified?

(b) Why does the thermal effect simply depend on the average vibration amplitude?

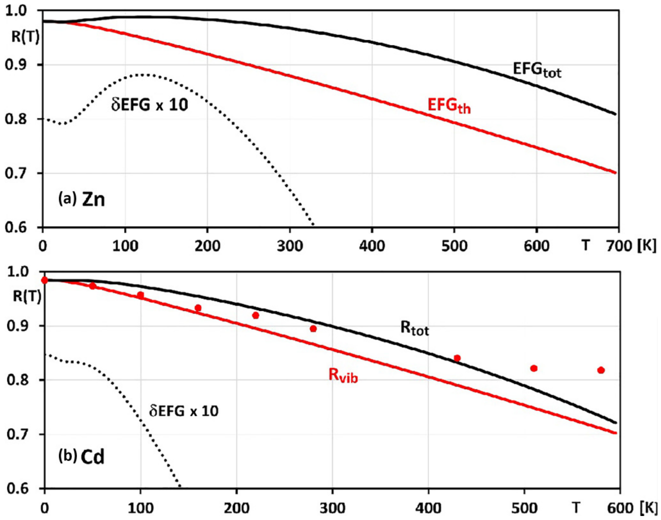

FIG. 5. EFG changes for (a) Zn and (b) Cd due to vibrational motion alone [$R_{\rm vib}$] and including the lattice effect. The pointed lines represent the shifts of the total result enlarged. The red points show the vibrational term for Cd extracted from [12] by substracting the structural contribution.

(c) Why does the thermal effect for the two separate matrices essentially have the same β'?

(d) Is a quantitative description of β' possible by a molecular dynamics approach?

A tentative explanation may be attempted:

(a) In principle the change of the lattice structure and the anharmonic terms in the vibrational amplitude have the same origin in the anharmonicity of the interatomic potentials in the solid. Since they both are taken from existing experimental data, and the leading term for their interdependence is included by the normalization of $B_{\rm av}$ to the atomic volume, only higher-order terms beyond a quasiharmonic treatment could devalidate the assumed separation.

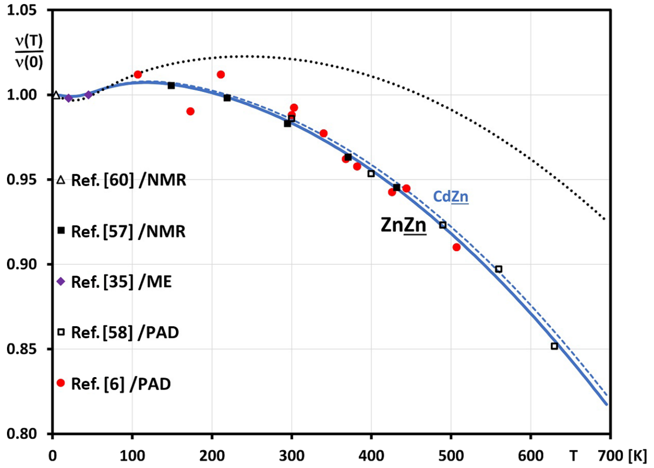

FIG. 6. Experimental data for Zn in Zn. The strong blue line shows the present fit, the dashed blue line that for Cd in Zn as comparison. Note the scatter of the PAD data below 350 K. The dotted black line is the result for the vibrational effect calculated in [13] augmented with the present structural contribution.

(b) This assumption, used as well in an early treatment [7], can in the present context only be tested by a comparison with experiment. In principle one would have to include another contribution dependent on the anisotropic vibration amplitude as sketched above, multiplied by another proportionality parameter β'_{an}. The data for Zn, however, show that such a term can only make a small contribution. Treating this contribution as the dominant one, as suggested in [13], is clearly excluded by the misfit to the data obvious in Fig. 4(a).

(c) This similarity is of course only possible using B_{av} renormalized to the atomic volume. It is then a natural consequence of the fact that the dependence of the EFG on atomic structure for the two metals is of the same nature. One can also see this in the similarity of their volume and c/a contributions to the EFG as documented above.

(d) Molecular dynamics calculations for the case of Cd [12] are fortunately available to answer this question. The extracted values of the vibrational contribution to the EFG change for several temperatures are included in Fig. 5(b). They virtually coincide with the present treatment in the low-temperature region up to 150 K. The calculated zero-point shift of the EFG, another effect directly proportional to β', is also practically identical to the result of the present work.

One could evidently apply the present approach to some other simple s-p metals. Obvious candidates would be Mg, Be, Hg, Sn, In, and Tl, where the only structural effect comes from the lattice parameters changing with temperature. For none of these, however, are the necessary experimental data for structure, vibrational amplitude, or EFG(T) as precise as for Zn. Furthermore, all (with the exception of Hg) are structurally more isotropic than Zn and Cd. This results in smaller EFGs and consequently even more critical interdependence of the various uncertainties. A similar treatment for metals that requires the knowledge of internal atomic position parameters as Ga, As, Sb, or Bi, even though precision EFG(T) data are available, is realistically excluded in the present situation for a theoretical analysis.

VIII. COMPARISON WITH EARLIER TREATMENTS

The first theoretical treatment of the EFG temperature dependence in some noncubic metals was presented in [7] and was virtually unchanged in [8]. The basic concept used has several aspects similar to the present work, in particular, the inclusion of the theoretically calculated lattice structure effect and the proportionality of the vibrational effects to the Debye-Waller factor. Since at the time no really advanced theoretical description of the EFG from first principles was available, a treatment using screened pseudopotentials had to be made. In addition, a much more simplified approximation of the atomic vibration amplitudes proportional to $T^{3/2}$ has been used. The reasonable agreement obtained with the then available experimental data, however, was quite promising. Unfortunately, the details of this work have never been made available. The announced calculational proof for ignoring the anisotropic vibration amplitudes, in particular, has never appeared.

The really *ab initio* treatment for the case of Cd [12], including a calculation also of the vibrational amplitudes as a function of temperature, was the first application of modern computational methods to the present problem. Unfortunately, the effect of the lattice structure temperature dependence was somewhat hidden in the treatment. It is a promising fact that the calculated vibrational effects at low temperature and the zero-point shift agree well with the results now obtained from experiment, as demonstrated in Fig. 5(b).

Both cases, Zn and Cd, were treated by a different *ab initio* procedure in [13], using experimental information for lattice vibration amplitudes. Unfortunately, these data (for Cd) as well as the ν_Q information (for Zn) assumed they are quite different from the ones arrived at in the present analysis. The conclusion that only the anisotropic part of B creates the EFG temperature dependence is completely opposite to the treatment in the present work, as demonstrated in Fig. 4(a). That their results appear to confirm the empirical $T^{3/2}$ relation may also be traced to the fact that the experimentally known lattice structure change with temperature is ignored. That also the addition of the now calculated structural effect does not bring their results into even approximate agreement with experiment, however, is demonstrated by the black dotted curve in Fig. 6 for Zn.

IX. IMPLICATION FOR NUCLEAR QUADRUPOLE MOMENTS I

Originally, one reason to start the present detailed analysis of the EFG temperature dependence for Zn was to obtain a better nuclear quadrupole moment for the $9/2^+$ state in ^{67}Zn, as its ν_Q data come from a PAD experiment and are thus only precise at higher temperatures. Having an improved understanding of EFG(T) would then allow a reliable extrapolation to 4 K, where Mössbauer data for the $5/2^-$ ground state with now reasonably well-known Q [28] have been available for a long time.

During the course of the present research, however, it was noted that another, more direct route exists to determine the ratio of the two quadrupole moments with rather good precision. In [57] ν_Q for the ^{67}Zn ground state had been measured using NMR in the temperature range from 149 to 431 K. Since in the temperature region around 400 K the results of the PAD experiments for the $9/2^+$ state show no sign of the effects of implantation damage and may thus be considered reliable, the ratio of $Q(9/2^+)$ to $Q(5/2^-)$ may be calculated quite accurately by combining the NMR frequencies with the average one of the two PAD measurements [58,6]. As result one obtains 3.774(20). Using the recently redetermined quadrupole moment for the ^{67}Zn ground state, $Q = 0.122(4)$ b [28,29], results in $Q = 0.46(2)$ b for the $9/2^+$ excited state, considerably smaller and more accurate than the previous value of 0.54(5) b [59]. With the interaction frequency from another high-precision NMR experiment [60] of $\nu_Q = 12.19(2)$ MHz at 4 K and very slightly renormalized data from Mössbauer spectroscopy [35] between 4 and 50 K, one thus also has a very useful data set $q(T)/q(0)$ for the pure Zn system.

All data assembled in Fig. 6 show practically the same temperature dependence as for Cd in Zn, the fitted factor of $\beta\prime = 0.483$ being identical within reasonable error. This behavior thus also conforms with the assumption made in analyzing the Cd in Zn data above, just using a relative EFG structural effect calculated for pure Zn.

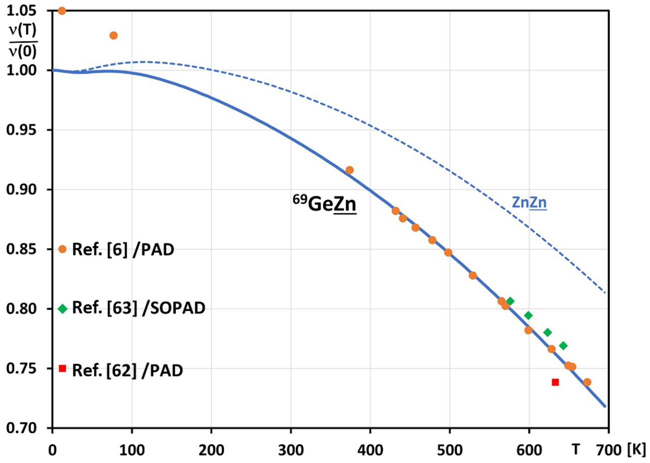

FIG. 7. Experimental data for ^{69}Ge in Zn. The strong blue line shows the present fit, the dashed blue line that for Zn in Zn as comparison. The PAD data below 350 K are clearly unreliable.

The obtained ν_Q for static conditions of the ^{67}Zn ground state, corrected for the calculated zero-point vibration effect of 2.2%, is $\nu_Q(0, \text{st}) = 12.46(3)$ MHz. This correction is very close to the one arrived at in [28] using different reasoning. Albeit small, it has to be taken into account when Q is obtained from precision DF calculations for the matrix.

X. IMPLICATION FOR NUCLEAR QUADRUPOLE MOMENTS II

One system where the existing data for ν_Q at high temperatures obtained by PAD are reasonably precise to allow an attempt of extrapolation to zero T is for the $9/2^+$ state of ^{69}Ge in Zn between 375 and 675 K. The present treatment has been applied to this case with the assumption that the structural contribution to the EFG for this impurity case is identical to the one for Zn in Zn. Clearly this is only a rough approximation, but more realistic density-functional calculations for this impurity case, though in principle possible, would require a rather extended computational effort. In addition to the lattice parameter changes the accompanying lattice relaxation around the impurity Ge would have to be treated as a function of temperature, using supercell calculations as done for the $T = 0$ structures in [32].

Figure 7 shows the obtained fit to the data with $\beta' = 0.66$, quite different from the case for the pure matrix. The strong increase relative to the pure matrix β' points to increased vibrational motion due to the Ge impurity. As a caveat one should note that for this case an advanced calculation of the structural contribution $R_{\text{str}}(T)$ mentioned above might also play a role. An even more extreme case of this behavior is known for Kr in Zn and Cd [61], and is not really understood yet. The scatter between the three different experiments in the highest-temperature region [6,62,63], visible in Fig. 7, can presumably be attributed to the inaccuracy of the temperature determination, inherent to the PAD technique. The two data points at 12 and 77 K show a very large frequency spread and can thus safely be ignored.

The value for $\nu_Q(0)$ obtained in this way is 96.3 MHz, to be confronted with 102 MHz from a fit assuming proportionality to $T^{3/2}$. Corrected for a calculated zero-point shift of 2.8% one obtains a static value of $\nu_Q(0, \text{st}) = 99.0$ MHz.

A rather early theoretical calculation for the EFG at *s*-*p* impurities in Zn and Cd including lattice relaxation effects [32] has predicted a ratio of 1.74 for the EFG of Ge in Zn relative to that of pure Zn. Using this value and the $\nu_Q(0, \text{st})$ for ^{67}Zn calculated above, one obtains $Q = 0.57(4)$ b for the ^{69}Ge $(9/2^+)$ state, with the estimated error coming primarily from the theoretical EFG ratio. For comparison, the previous value is 0.75(8) b [59]. Obviously, this also changes the values of Q for ^{67}Ge $(9/2^+)$, ^{71}Ge $(5/2^+)$ [62], and ^{73}Ge $(5/2^+)$ [64], related to it by comparatively accurate frequency ratios.

XI. OTHER IMPURITY SYSTEMS

There exist very many measurements of the temperature dependence for the nuclear quadrupole interaction at impurity nuclei in the strongly anisotropic simple *s*-*p* metals Zn, Cd, and Hg. Unfortunately, most of these have been performed using the PAD technique and are at best reliable at temperatures above half the melting point, thus much reducing their usefulness for a quantitative analysis. An exception are the very early PAC measurements for In in Zn [65] and Cd [66]. Repeating these studies, unfortunately of somewhat limited precision, with present day PAC techniques would offer the possibility to test the approach in the present work also for the impurity EFG in a quantitative way.

XII. IMPLICATIONS FOR FUTURE WORK

It would obviously be of considerable interest to have very precise data for the EFG temperature dependence over the full temperature range. In the case of Zn this would in principle be possible using the NQR technique. Such an attempt, unfortunately, has in the early period of such measurements [67] produced a result inconsistent with later Mössbauer effect and NMR work [35,60]. This possibility would, in particular, be relevant for testing the predictions of the present analysis for the small deviations in the low-temperature range, as indicated by the dotted curve in Fig. 5(a). For Cd, on the other hand, NQR is not possible, and, though somewhat more precise PAC data could certainly still be obtained, the interesting temperature region below 50 K appears technically hard to reach, in particular, considering the difficulties in reproducibly producing sources for ^{111}In in Cd, as observed in [14].

A fully parameter-free theoretical calculation of the type performed for Cd [12] also for Zn would obviously be valuable in corroborating the present analysis, at least in the low-temperature region. It would be difficult, however, to imagine an outcome for the β' parameter deviating from the one found here.

Clearly, a somewhat uncertain aspect of the present work is the necessity to use a theoretical Debye-Waller factor for Cd, at least in the high-temperature region. A proper measurement of this over the full temperature range would thus be highly desirable, the available information to date being completely inconsistent [see Fig. 3(b)]. Such an endeavor would involve a considerable effort, however, since also for the technically much easier case of Zn there are still some minor inconsistencies.

XIII. GENERAL CONCLUSIONS

The present work has demonstrated the close relation of the motional vibrational amplitudes (DWF) in the simple metals Zn and Cd with the corresponding temperature dependence of the EFG. Though there is still some theoretical work needed to exactly quantify this relationship for other noncubic metals, the approach presented here offers the possibility to obtain the DWF via a quantity that is determined through a frequency measurement, not the traditionally needed intensity or width measurement of diffraction peaks.

For other simple systems, cubic MX_3 alloys as a possible example, the temperature dependence of the EFG as a local property could eventually serve as a means to get information on the local vibration amplitudes, otherwise only obtainable for a few isolated cases from Mössbauer effect spectroscopy.

ACKNOWLEDGMENTS

The author would like to thank J. G. Correia and V. S. Amaral for critical reading of the manuscript and also J. G. Correia for converting graphical information into digital data. This work was developed within the scope of the project CICECO-Aveiro Institute of Materials, UIDB/50011/2020 (DOI 10.54499/UIDB/50011/2020), UIDP/50011/2020 (DOI 10.54499/UIDP/50011/2020) & LA/P/0006/2020 (DOI 10.54499/LA/P/0006/2020), financed by national funds through the FCT/MCTES (PIDDAC).

---

[1] H. G. Dehmelt and H. Krüger, Quadrupol-resonanzfrequenzen von Cl- und Br-kernen in kristallinem dichloräthylen und methylbromid, Z. Phys. **129**, 401 (1951).

[2] H. Bayer, Zur theorie der spin-gitterrelaxation in molekülkristallen, Z. Phys. **130**, 227 (1951).

[3] P. Raghavan and R. S. Raghavan, Nuclear quadrupole interaction in cadmium metal, Phys. Rev. Lett. **27**, 724 (1971).

[4] J. Bleck, R. Butt, H. Haas, W. Ribbe, and W. Zeitz, In-beam measurements of the nuclear quadrupole interaction in cadmium metal, Phys. Rev. Lett. **29**, 1371 (1972).

[5] R. Vianden, Electric field gradients in metals, Hyperfine Interact. **35**, 1077 (1987).

[6] J. Christiansen, P. Heubes, R. Keitel, W. Klinger, W. Loeffler, W. Sandner, and W. Witthuhn, Temperature dependence of the electric field gradient in noncubic metals, Z. Phys. B **24**, 177 (1976).

[7] K. Nishiyama, F. Dimmling, T. Kornrumpf, and D. Riegel, Theory of the temperature dependence of the electric field gradient in noncubic metals, Phys. Rev. Lett. **37**, 357 (1976).

[8] K. Nishiyama and D. Riegel, Recent developments in the analysis of electric field gradients in metals, Hyperfine Interact. **4**, 490 (1978).

[9] P. Jena and J. Rath, *Ab initio* calculation of the temperature dependence of the electric field gradient in Be, Phys. Rev. B **23**, 3823 (1981).

[10] P. Blaha, K. Schwarz, and P. H. Dederichs, First-principles calculation of the electric-field gradient in hcp metals, Phys. Rev. B **37**, 2792 (1988).

[11] P. Blaha, P. Dufek, K. Schwarz, and H. Haas, Calculation of electric hyperfine interaction parameters in solids, Hyperfine Interact. **97-98**, 1 (1996).

[12] D. Torumba, K. Parlinski, M. Rots, and S. Cottenier, Temperature dependence of the electric-field gradient in hcp-Cd from first principles, Phys. Rev. B **74**, 144304 (2006).

[13] A. V. Nikolaev, N. M. Chtchelkatchev, D. A. Salamatin, and A. V. Tsvyashchenko, Towards an *ab initio* theory for the temperature dependence of electric field gradients in solids: Application to hexagonal lattices of Zn and Cd, Phys. Rev. B **101**, 064310 (2020).

[14] L. Hermans, J. van Cauteren, and M. Rots, Anomalous low temperature behavior of the electric field gradient at ^{111}Cd in cadmium and zinc, Phys. Lett. A **108**, 210 (1985).

[15] P. Raghavan, R. S. Raghavan, E. N. Kaufmann, K. Krien, and R. A. Naumann, Nuclear quadrupole interaction of ^{111}Cd in zinc (by PAC), J. Phys. F **4**, L80 (1974).

[16] R. Feder and A. S. Nowick, Dilatometric and x-ray thermal expansion in non cubic crystals. II. Experiments on cadmium, Phys. Rev. B **5**, 1244 (1972).

[17] B. Zhang, X. Li, and D. Li, Assessment of thermal expansion coefficients for pure metals, CALPHAD **43**, 7 (2013).

[18] V. Y. Bodryakov, Joint study of temperature dependence of thermal expansion and heat capacity of solid beryllium, High Temp. **56**, 177 (2018).

[19] V. Y. Bodryakov and Y. N. Babintsev, Correlation analysis of the heat capacity and thermal expansion of solid mercury, Phys. Solid State **57**, 1264 (2015).

[20] Y. S. Touloukian, R. K. Kirby, R. E. Taylor, and D. D. Desai, Thermal expansion, metallic elements and alloys, TPRC Data Series **12**, 1 (1975).

[21] R. D. McCammon and G. K. White, Thermal expansion at low temperatures of hexagonal metals: Mg, Zn and Cd, Philos. Mag. **11**, 1125 (1965).

[22] J. Nuss, U. Wedig, A. Kirfel, and M. Jansen, The structural anomaly of zinc: Evolution of lattice constants and parameters of thermal motion in the temperature range of 40 to 500 K, Z. Anorg. Allg. Chem. **636**, 309 (2010).

[23] P. D. Pathak and R. J. Desai, Thermal properties of some hcp metals. I. Thermal expansion of zinc and cadmium, Phys. Status Solidi A **62**, 625 (1980).

[24] R. W. Meyerhoff and J. F. Smith, Anisotropic thermal expansion of single crystals of thallium, yttrium, beryllium, and zinc at low temperatures, J. Appl. Phys. **33**, 219 (1962).

[25] P. Blaha, K. Schwarz, G. K. H. Madsen, D. Kvasnicka, and J. Luitz, *WIEN2K: An Augmented Plane Wave Plus Local Orbitals Program for Calculating Crystal Properties* (Vienna University of Technology, Vienna, 2001).

[26] J. P. Perdew, K. Burke, and M. Ernzerhof, Generalized gradient approximation made simple, Phys. Rev. Lett. **77**, 3865 (1996).

[27] J. Bieron, L. Filippin, G. Gigalas, M. Godefroid, P. Jönsson, and P. Pyykkö, *Ab initio* calculations of the hyperfine structure of zinc and evaluation of the nuclear quadrupole moment $Q(^{67}\mathrm{Zn})$, Phys. Rev. A **97**, 062505 (2018).

[28] H. Haas, S. P. A. Sauer, L. Hemmingsen, V. Kellö, and P. W. Zhao, Quadrupole moments of Cd and Zn nuclei: When

solid-state, molecular, atomic, and nuclear theory meet, Europhys. Lett. **117**, 62001 (2017).

[29] H. Haas, J. Röder, J. G. Correia, J. Schell, A. S. Fenta, R. Vianden, E. M. H. Larsen, P. A. Aggelund, R. Fromsejer, L. B. S. Hemmingsen, S. P. A. Sauer, D. C. Lupascu, and V. S. Amaral, Free molecule studies by perturbed gamma-gamma angular correlation: A new path to accurate nuclear quadrupole moments, Phys. Rev. Lett. **126**, 103001 (2021).

[30] F. Tran and P. Blaha, Implementation of screened hybrid functionals based on the Yukawa potential within the LAPW basis set, Phys. Rev. B **83**, 235118 (2011).

[31] H. Haas, M. B. Barbosa, and J. G. Correia, The quadrupole moments of Cd and Zn isotopes—an apology, Hyperfine Interact. **237**, 115 (2016).

[32] H. Haas and J. G. Correia, The EFG at *sp*-impurities in Zn and Cd—a new (final?) look, Hyperfine Interact. **197**, 11 (2010).

[33] G. Schatz, E. Dafni, H. H. Bertschat, C. Broude, F. D. Davydovsky, and M. Hass, Electric quadrupole interaction of 192Tl(8^-) nuclei in hexagonal Tl and in tetragonal In metals, Z. Phys. B **49**, 23 (1982).

[34] L.-M. Peng, G. Ren, S. L. Dudarev, and M. J. Whelan, Debye-Waller factors and absorptive scattering factors of elemental crystals, Acta Cryst. A **52**, 456 (1996).

[35] W. Potzel, W. Adlassnig, U. Närger, Th. Obenhuber, K. Riski, and G. M. Kalvius, Temperature dependence of hyperfine interactions and anisotropy of recoil-free fraction: A Mössbauer study of the 93.3 keV resonance of ^{67}Zn in single crystals of zinc metal, Phys. Rev. B **30**, 4980 (1984).

[36] P. D. Pathak and R. J. Desai, Thermal properties of some hcp metals. II. Debye-Waller factors of zinc, cadmium and magnesium, Phys. Status Solidi A **64**, 741 (1981).

[37] S. P. Tewari and P. Silotia, The effect of crystal anisotropy on the Lamb Mössbauer recoilless fraction and second-order Doppler shift in zinc, J. Phys.: Condens. Matter **1**, 5165 (1989).

[38] N. G. Krishna and D. B. Sirdeshmukh, Compilation of temperature factors of hexagonal close packed elements, Acta Cryst. A **54**, 513 (1998).

[39] E. Rossmanith, X-ray measurement of the root-mean-square displacement of atoms in zinc single crystals. A case of high anisotropic extinction, Acta Cryst. A **33**, 593 (1977).

[40] R. Tomaschitz, Thermodynamics of lattice vibrations in non-cubic crystals: The zinc structure revisited, Acta Cryst. A **77**, 420 (2021).

[41] E. F. Skelton and J. L. Katz, Examination of the thermal variation of the mean square atomic displacements in zinc and evaluation of the associated Debye temperature, Phys. Rev. **171**, 801 (1968).

[42] A. Togo and I. Tanaka, First principles phonon calculations in materials science, Scr. Mater. **108**, 1 (2015).

[43] S. Narasimham and S. de Gironcoli, *Ab initio* calculation of the thermal properties of Cu: Performance of the LDA and GGA, Phys. Rev. B **65**, 064302 (2002).

[44] J. Xie, S. P. Chen, S. de Gironcoli, and S. Baroni, Thermodynamic properties and lattice dynamics of silver at high pressure: A first-principles study, Philos. Mag. B **79**, 911 (1999).

[45] H. X. Gao and L.-M. Peng, Parametrization of the temperature dependence of the Debye-Waller factors, Acta Cryst. A **55**, 926 (1999).

[46] J. A. Young and J. U. Koppel, Lattice vibrational spectra of beryllium, magnesium, and zinc, Phys. Rev. **134**, A1476 (1964).

[47] L. Almquist and R. Stedman, Phonons in zinc at 80 K, J. Phys. F **1**, 785 (1971).

[48] G. Toussaint and G. Champier, Lattice dynamics of cadmium at 88 K, Phys. Status Solidi B **54**, 165 (1972).

[49] C. Kittel, in *Introduction to Solid State Physics*, 8th ed. (John Wiley & Sons, New York, 2005), p. 116.

[50] Y. Watanabe, H. Iwasaki, and S. Ogawa, An x-ray investigation of thermal mean-square atomic displacements in magnesium, cadmium and Mg_3Cd, Jpn. J. Appl. Phys. **10**, 786 (1971).

[51] E. Rossmanith, Lindemann's rule and the x-ray Debye temperature of anisotropic Zn and Cd single crystals, Acta Cryst. A **35**, 243 (1979).

[52] C. Mallica and A. Dal Corso, Temperature-dependent atomic *B* factor: An *ab initio* calculation, Acta Cryst. A **75**, 624 (2019).

[53] B. Dorner, A. A. Chernyshov, V. V. Pushkarev, A. Yu Rumyantsev, and R. Pynn, Phonons in cadmium at 80 K, J. Phys. F **11**, 365 (1981).

[54] R. Keitel, W. Engel, H. Föttinger, D. Forkel, M. Iwatschenko-Borho, F. Meyer, and W. Witthuhn, Point defects in the hcp metals Cd and Zn, Hyperfine Interact. **15**, 425 (1983).

[55] R. S. Raghavan and P. Raghavan, Anomalous temperature dependence of the quadrupole interaction in cadmium, Phys. Lett. A **36**, 313 (1971).

[56] T. Butz, B. Lindgren, and H. Saitovich, The effect of lattice vibrations on the pressure dependence of the electric field gradient in cadmium metal, Hyperfine Interact. **7**, 81 (1979).

[57] T. J. Bastow, ^{67}Zn NMR in zinc metal, J. Phys.: Condens. Matter **8**, 11309 (1996).

[58] H. Bertschat, E. Recknagel, and B. Spellmeyer, Temperature-dependent electric quadrupole interaction of ^{67}Zn in zinc metal, Phys. Rev. Lett. **32**, 18 (1974).

[59] N. J. Stone, Table of nuclear electric quadrupole moments, At. Data Nucl. Data Tables **111-112**, 1 (1916).

[60] J. Goyette and R. V. Pound, Electric quadrupole interaction of ^{67}Zn in zinc metal, Phys. Rev. B **35**, 391 (1987).

[61] H. Haas and H. H. Bertschat, Temperature dependence of EFG for krypton in Zn and Cd, Hyperfine Interact. **9**, 273 (1976).

[62] H. Haas, W. Leitz, H.-E. Mahnke, W. Semmler, R. Sielemann, and Th. Wichert, Quadrupole interaction of Ge nuclei in Zn and Ga following nuclear reactions, Phys. Rev. Lett. **30**, 656 (1973).

[63] G. Schatz, R. Brenn, and D. B. Fossan, Stroboscopic observation of quadrupole hyperfine interactions, Phys. Lett. B **57**, 231 (1975).

[64] J. G. Correia, H. Haas, J. G. Marques, A. A. Melo, and J. C. Soares, ^{73}Ge: A new high resolution PAC probe, Hyperfine Interact. **80**, 1321 (1993).

[65] S. Devare, D. R. S. Somayajulu, and H. G. Devare, Quadrupole interaction of ^{117}In in Zn metal, Hyperfine Interact. **1**, 151 (1975).

[66] R. Butt, H. Haas, and S. Rosenblum, Temperature dependence of the electric field gradient of indium in cadmium, Phys. Rev. B **9**, 3705 (1974).

[67] E. N. Kaufmann, J. R. Brookeman, P. C. Canepa, T. A. Scott, D. H. Rasmussen, and J. H. Perepezko, Observation of pure quadrupole resonance in zinc metal, Solid State Commun. **29**, 375 (1979).